Journal of Applied Pharmaceutical Research
Volume 14 Issue 3, Year of Publication 2026, Page 380 – 390
DOI: https://doi.org/10.69857/joapr.v14i3.1977

Check for updates

Research Article

JOURNAL OF APPLIED PHARMACEUTICAL RESEARCH | JOAPR
www.japtronline.com *ISSN: 2348 – 0335*

DEVELOPMENT AND OPTIMIZATION OF ZINGERONE-LOADED PLGA OIL-BASED NANOCARRIERS FOR ENHANCED SOLUBILITY AND SUSTAINED DRUG RELEASE

Varsha Laxman Jakune[1*], Varsha Siddheswar Tegeli[2]

Article Information
Received: 10th January 2026
Revised: 2nd March 2026
Accepted: 19th April 2026
Published: 15th May 2026

Keywords
Zingerone, PLGA nanocarrier, peanut oil, sustained release, drug delivery, solubility enhancement.

ABSTRACT
Background: Zingerone, a phenolic constituent of *Zingiber officinale*, possesses notable antioxidant, anti-inflammatory, and anticancer activities. Its therapeutic use is limited by poor water solubility and low oral bioavailability, resulting in suboptimal efficacy. Polymeric nanocarriers, especially poly(lactic-co-glycolic acid) (PLGA)-based systems, offer an effective approach to enhance solubility, stability, and controlled drug delivery. Integration of lipid components into PLGA matrices can further improve drug loading and solubilization. This study focused on the design and optimization of zingerone-loaded PLGA oil-based nanocarriers to improve solubility and sustained release. **Methodology:** Solubility screening of zingerone in different oils identified peanut oil as the most suitable vehicle (54.31 mg/ml). Nanocarriers were prepared using a solvent evaporation method, producing nine formulations (F1–F9) with varying oil content and homogenization speeds. Characterization included particle size and zeta potential analysis, FTIR, DSC, SEM, and drug content determination using UV spectroscopy and HPLC. Drug release was studied using a dialysis membrane in phosphate buffer (pH 6.4), and stability testing was performed for the optimized formulation. **Results and Discussion:** The optimized batch (F4) exhibited a particle size of 79.7 nm, a zeta potential of −27.3 mV, and a drug content of 99.73%. Solubility increased more than 30-fold (5.44 mg/ml), with sustained drug release reaching 97.7% over 24 hours. Characterization confirmed efficient encapsulation and formulation stability. **Conclusion:** PLGA oil-based nanocarriers significantly improved zingerone solubility and enabled controlled release, indicating strong potential for further pharmacokinetic and therapeutic evaluation.

INTRODUCTION

Zingerone is a phenolic alkanone from ginger (*Z. officinale*) that has attracted research attention for its diverse pharmacological effects. These effects include anti-inflammatory, antioxidant, anticancer, & antimicrobial properties. However, zingerone's clinical applications are limited by its poor water solubility and low oral bioavailability. These issues lead to inadequate

[1]*Punyashlok Ahilyadevi Holkar Solapur University, Solapur-Pune National Highway, Kegaon, Solapur-413255, Maharashtra, India.*
[2]*D.S.T.S. Mandal's College of Pharmacy, Solapur-413255, Maharashtra, India.*

For Correspondence:** **vrs11jakune@gmail.com

systemic exposure & reduce the compound's effectiveness when taken in traditional forms [1-2]. To address these challenges, new drug delivery methods are needed. Systems based on nanotechnology, especially polymeric nanocarriers, offer a promising way to improve the solubility and bioavailability of drugs that are poorly soluble in water. Among the various polymers, poly(lactic-co-glycolic acid) (PLGA) has become a popular choice for nanocarrier fabrication [3]. This is due to its compatibility with biological systems, ability to break down naturally, and a proven track record of approval for pharmaceutical use. Adding lipophilic oils to PLGA in the design of nanocarriers can further enhance drug loading and solubilization, making these hybrid systems appealing for challenging compounds like zingerone [4]. Oil-loaded PLGA nanocarriers can significantly help overcome the solubility and permeability issues faced by hydrophobic natural substances [5-6]. These carriers not only enable greater drug encapsulation and controlled release but also help preserve the encapsulated compound's stability, protecting it from premature degradation. By adjusting factors such as particle size, surface charge, and release kinetics, PLGA-oil nanocarriers can be fine-tuned to meet specific therapeutic goals and extend their circulation in the bloodstream [7-9]. Given these benefits, this study aims to systematically develop and refine zingerone-loaded PLGA oil-based nanocarriers. The goal is to use these new delivery methods to improve the solubility, extend the release time, and increase the pharmacological potential of zingerone, ultimately facilitating its effective use in clinical or nutraceutical products. Previous approaches for enhancing zingerone bioavailability include lipid-based nanoemulsions, liposomes, and solid dispersions. However, these systems often suffer from limited physical stability or rapid drug release. In contrast, the present oil-integrated PLGA nanocarrier system provides a dual advantage of enhanced solubilization via lipid incorporation and sustained release via polymeric encapsulation, thereby offering improved formulation robustness and controlled delivery.

MATERIALS AND METHODS

Materials

Zingerone was procured from Sigma-Aldrich, India, PLGA from Evonik India Pvt. Ltd., Mumbai, and Poloxamer 188 from BASF India Ltd., Mumbai. Oils (olive oil, peanut oil, sesame oil) were purchased from Himedia Laboratories Pvt. Ltd., Mumbai, while isopropyl myristate & Capryol 90 were obtained from Gattefossé India Pvt. Ltd., Mumbai. Acetone, methanol & other analytical grade chemicals were supplied by Merck India Ltd., Mumbai.

PRELIMINARY DRUG ANALYSIS

Particle Size and Zeta Potential

The average particle size and zeta potential of the formulations were evaluated using a Horiba SZ-100 nanoparticle analyzer. All measurements were conducted at 25°C employing disposable sizing cuvettes. Prior to analysis, each sample was appropriately diluted with deionized water to ensure optimal dispersion. The refractive index, viscosity, and dielectric constant parameters were standardized across all measurements to maintain consistency [10].

Fourier-transform Infrared Spectroscopy (FTIR)

Molecular interaction studies were performed via FTIR spectroscopy. For each measurement, approximately 1–2 mg of the freeze-dried sample was intimately mixed with 100 mg of potassium bromide, then pelletized using a hydraulic press. The resulting pellet was examined over the wavelength range 400–4000 cm^-1 to identify characteristic functional groups [11].

Differential Scanning Calorimetry (DSC)

Thermal analysis was conducted using a Mettler-Toledo DSC instrument. About 1 mg of the sample was accurately weighed and sealed in a standard aluminum pan. After equilibrating at 25°C for 10 minutes, the sample was subjected to a controlled heating scan from 25°C to 300°C at a rate of 10 K/min. Thermograms were interpreted to assess any transitions or interactions [12].

Scanning Electron Microscopy (SEM)

Nanocarrier morphology and surface characteristics were observed using a Quanta Inspect F50 field-emission gun SEM operated at 30 kV. Dried samples were mounted onto stubs, coated with a conductive material as necessary, and imaged at various magnifications to examine particle uniformity and surface features [13].

PRE-FORMULATION STUDIES

Wavelength Selection

The maximum absorption wavelength (λmax) for zingerone was determined using UV–Visible spectrophotometry. A standard solution of zingerone (10 µg/ml) was prepared in phosphate buffer (pH 6.4) and scanned over 190-400 nm to determine the λmax for subsequent analyses.

Calibration Curves

Standard calibration curves were constructed in both methanol (concentration range: 0–60 µg/ml) and phosphate buffer (pH 6.4;

range: 0–50 µg/ml). Absorbance readings were recorded at the respective λmax values, enabling precise quantification in subsequent experiments [14].

Saturation Solubility

To assess oil suitability, an excess of zingerone was added to 5 mL of each candidate oil. Samples were mixed overnight at room temperature using a mechanical shaker, then centrifuged at 2500 rpm for 20 minutes. The clear supernatant was diluted with methanol and analyzed spectrophotometrically to determine dissolved drug concentration [15].

Preparation of Nanocarriers

The solvent evaporation technique was employed for nanocarrier formulation. A fixed amount of zingerone and peanut oil was dissolved in acetone, and PLGA was gradually incorporated into the solution. The resulting organic phase was added dropwise to an aqueous phase containing 0.5% (w/v) Poloxamer 188 while stirring continuously. The emulsion was homogenized at predefined speeds (5000–10000 rpm) for 30 minutes, employing an ice bath to control temperature (Table 1). The mixture was then stirred overnight to evaporate the organic solvent. Formed nanocarriers were isolated by filtration and dried at room temperature. Nanocarriers were isolated using membrane filtration (0.22 µm pore size). However, considering the nanoscale size range, recovery efficiency was ensured by combining filtration with centrifugation at 15,000 rpm for 20 minutes to minimize particle loss [16].

Formulation Design

Nine distinct batches (F1–F9) were produced by systematically varying peanut oil content (100–300 mg) and homogenization speeds (5000–10000 rpm), while amounts of zingerone (20 mg), PLGA (200 mg), acetone (15 ml), Poloxamer 188 (500 mg), and water (100 ml) remained constant. Homogenization was maintained for 30 minutes in all formulations (Table 1).

Table 1: Formulation Table for Zingerone PLGA oil based Nanocarrier

Ingredients	F1	F2	F3	F4	F5	F6	F7	F8	F9
Zingerone (mg)	20	20	20	20	20	20	20	20	20
Peanut oil (mg)	100	300	200	100	300	200	200	100	300
PLGA (mg)	200	200	200	200	200	200	200	200	200
Acetone (ml)	15	15	15	15	15	15	15	15	15
Poloxamer 188 (mg)	500	500	500	500	500	500	500	500	500
Water (ml)	100	100	100	100	100	100	100	100	100
Homogenization Speed (rpm)	10000	10000	7500	5000	5000	5000	10000	7500	7500
Homogenization Time (minutes)	30	30	30	30	30	30	30	30	30

EVALUATION OF NANOCARRIERS

Particle Size and Zeta Potential

Prepared nanocarriers were redispersed in deionized water and re-evaluated using identical methods as in the preliminary drug analysis.

Drug Content

The encapsulated drug was quantified by dissolving an accurately weighed amount of nanocarrier in methanol. Absorbance was measured at 282 nm using a UV–Vis spectrophotometer or chromatographically via HPLC on a Luna C18 column set to 282 nm. Results were calculated using established calibration curves [17].

In Vitro Release Studies

Drug release kinetics were probed using a dialysis bag technique. A formulation equivalent to 5 mg zingerone was sealed in a dialysis membrane and immersed in 200 mL of phosphate buffer (pH 6.4) at 37°C. At predefined time points, aliquots of the release medium were withdrawn, replaced with fresh buffer, and analyzed spectrophotometrically to determine zingerone concentration. A phosphate buffer at pH 6.4 was selected to simulate intestinal conditions where zingerone absorption is expected, ensuring relevance to oral delivery systems [18].

Saturation Solubility of Nanocarriers

To further assess the improvement in solubilization, the saturation solubility of both the pure drug and the final nanocarrier formulation was measured in water after overnight mixing using the previously described spectrophotometric method [19].

Stability Studies

For stability evaluation, the optimal nanocarrier batch was stored under appropriate conditions. After the storage period, samples

were analyzed for physicochemical attributes—including FTIR profiles, DSC thermograms, particle size, zeta potential, drug content, and in vitro release using the approaches outlined above [20]. All experiments were performed in triplicate (n = 3), and results are expressed as mean ± standard deviation (SD).

RESULTS AND DISCUSSION
PRELIMINARY DRUG ANALYSIS

Particle Size and Zeta Potential

Dynamic light scattering (DLS) measurements of pure zingerone revealed an average hydrodynamic diameter of 97.13 ± 11.50 nm, with the particle size distribution spanning from 79.7 nm to 113.9 nm. The corresponding zeta potential analysis showed moderately negative surface charges, ranging between –19.8 mV and –27.3 mV across independent batches. The negative surface charge indicates electrostatic repulsion among dispersed particles, which is generally associated with colloidal stability and the prevention of aggregation (Figures 1 & 2). The reported hydrodynamic diameter represents aggregated structures formed in aqueous dispersion rather than the intrinsic molecular size of zingerone.

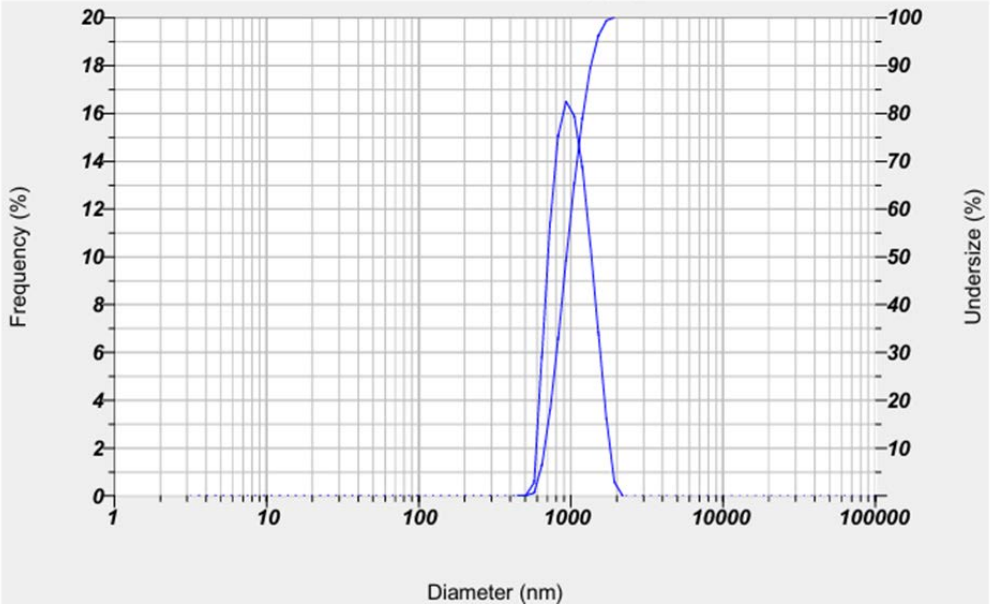

Figure 1: Particle size distribution of Zingerone

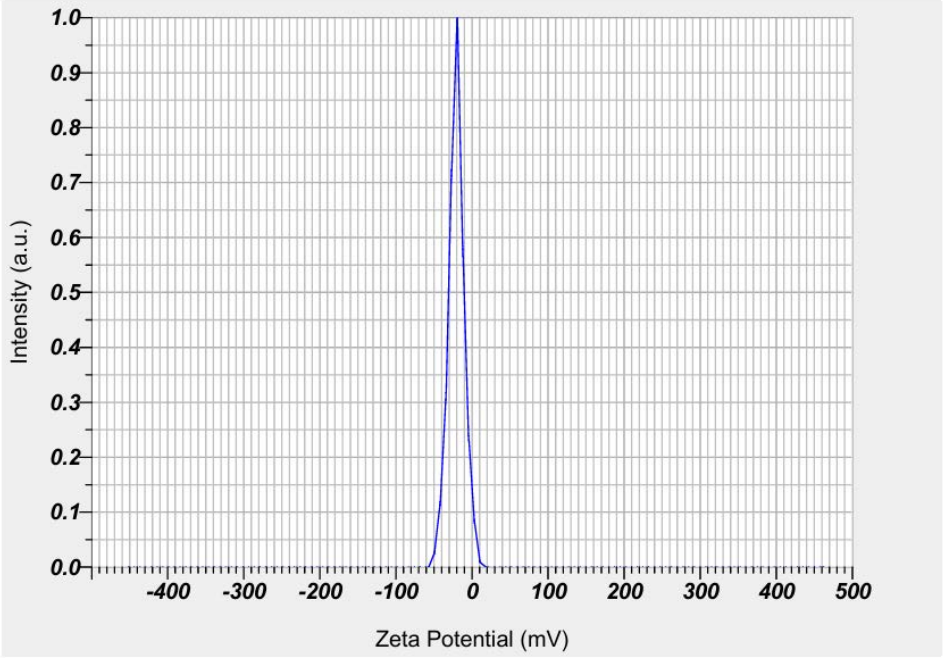

Figure 2: Zeta potential of Zingerone

Fourier Transform Infrared Spectroscopy (FTIR)

The FTIR spectrum of pure zingerone exhibited distinct absorption peaks at approximately 3430 cm^{-1} (O–H stretching), 1670 cm^{-1} (C=O stretching of carbonyl groups), and ~3020 cm^{-1} (aromatic C–H stretching), consistent with its functional groups (Figure 3). When analyzed in the optimized nanocarrier formulation F4, these characteristic peaks were retained with only minor shifts in position, suggesting the preservation of the drug's chemical structure. The absence of significant peak disappearance or new band formation confirmed that no major chemical interactions occurred between zingerone, peanut oil, and PLGA during formulation.

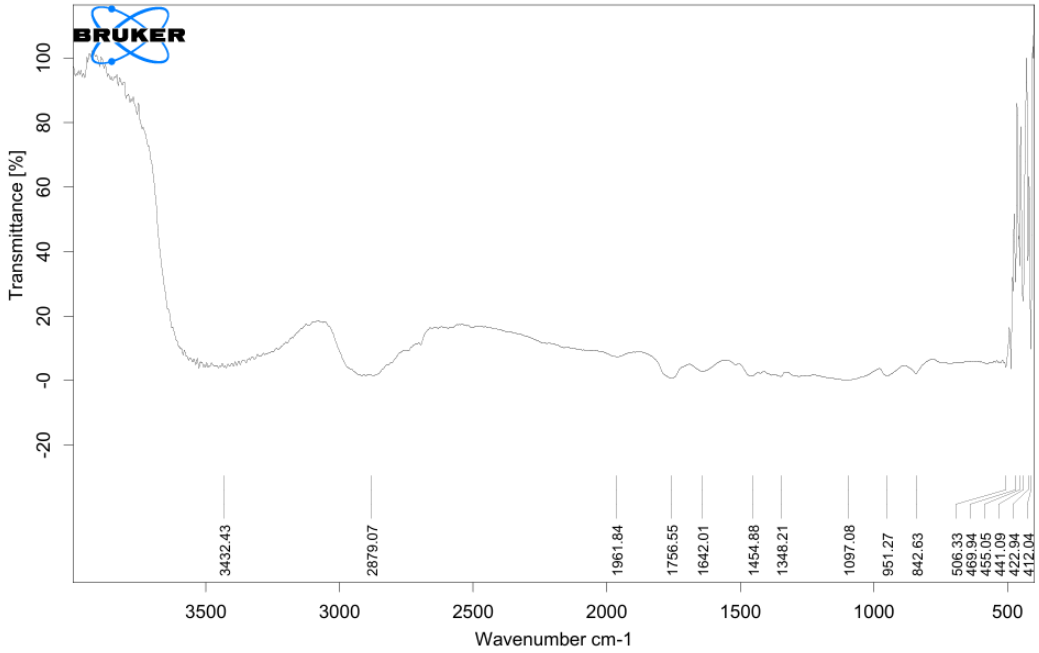

Figure 3: FTIR of Batch F4

Differential Scanning Calorimetry (DSC)

The DSC thermogram of pure zingerone displayed a sharp endothermic peak around its melting point, confirming its crystalline nature (Figure 4). In contrast, DSC analysis of optimized formulation F4 demonstrated broadened and reduced intensity endothermic transitions. This alteration indicates a partial loss of crystallinity and a shift toward a more amorphous state in zingerone, suggesting homogeneous molecular dispersion of the drug within the polymer matrix.

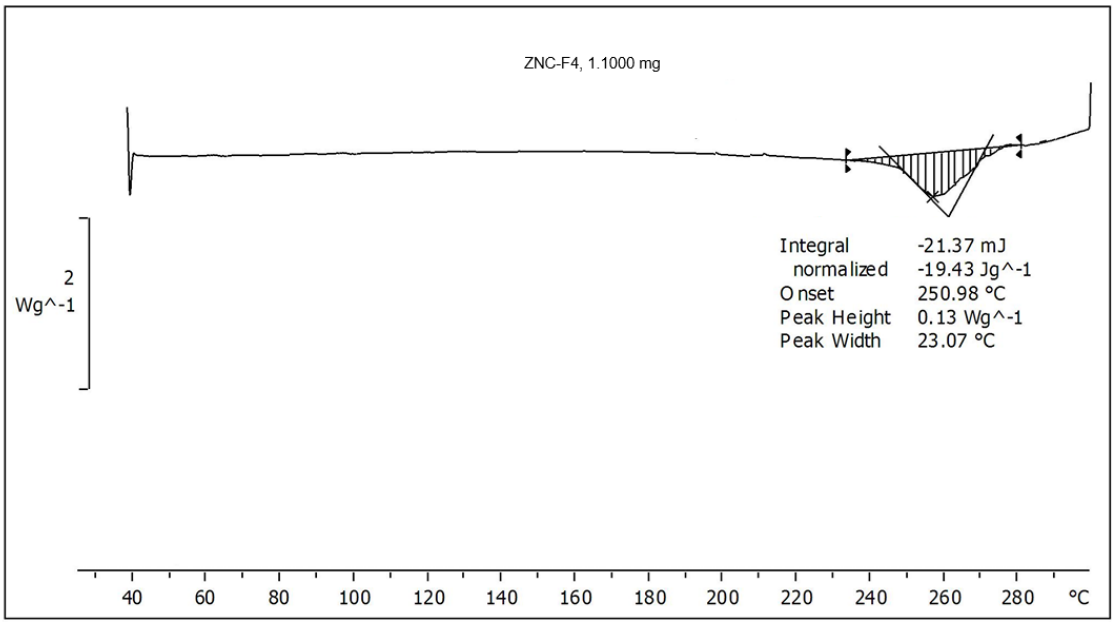

Figure 4: DSC of Batch F4

Scanning Electron Microscopy (SEM)

SEM micrographs revealed that the developed nanocarriers exhibited a predominantly spherical morphology with uniform size distribution (Figures 5a & 5b).

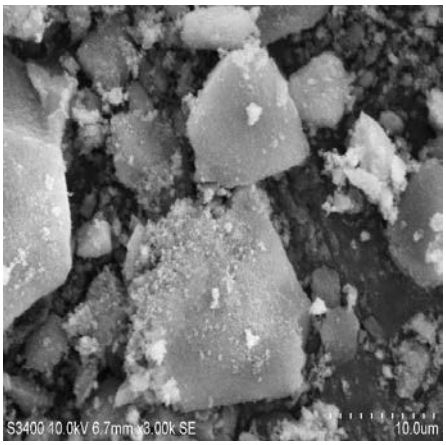

Figure 5: SEM of a) Pure Drug Zingerone

The particle surfaces appeared smooth and free of visible drug crystals, further validating successful encapsulation of zingerone within the PLGA matrix.

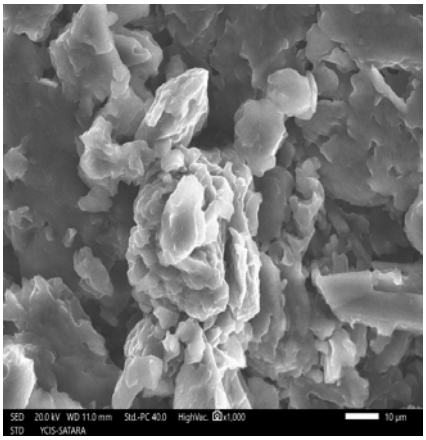

Figure 5: SEM of b) Batch F4

PREFORMULATION STUDIES

Wavelength Selection and Calibration Curve

The maximum absorbance wavelength (λmax) of zingerone in phosphate buffer (pH 6.4) was found to be 282 nm (Figure 6). Calibration curves were established in methanol (0–60 µg/mL) and phosphate buffer (0–50 µg/mL), both of which demonstrated excellent linearity with correlation coefficients (R^2 > 0.99) (Tables 3; Figures 7 & 8). These findings confirmed the reliability and reproducibility of spectrophotometric methods for quantitative analysis of zingerone.

Table 3: Calibration data showing linearity of zingerone in methanol and phosphate buffer (pH 6.4) at λmax 282 nm

Conc. (µg/mL)	Absorbance (Methanol)	Conc. (µg/mL)	Abs. (Phosphate Buffer pH 6.4)
0	0.000	0	0.000
12	0.175	10	0.171
24	0.379	20	0.372
36	0.591	30	0.551
48	0.783	40	0.755
60	0.990	50	0.956

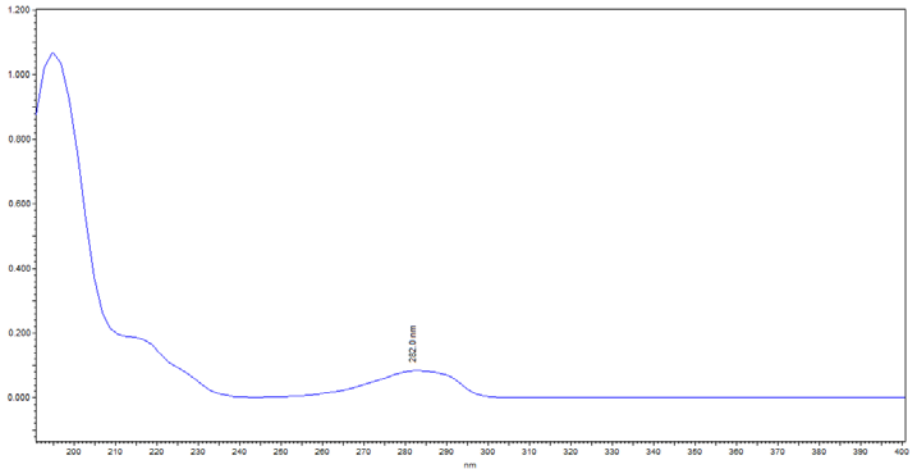

Figure 6: UV Spectrum of Zingerone

Saturation Solubility Studies

The solubility profile of zingerone was determined in various oils. Among the tested candidates, peanut oil demonstrated the highest solubility (54.31 mg/mL), followed by isopropyl myristate (44.34 mg/mL) and olive oil (26.68 mg/mL). Sesame oil exhibited the lowest solubility at 17.96 mg/mL (Table 4). Considering these findings, peanut oil was selected as the oil phase for nanocarrier formulation owing to its superior solubilizing capacity for zingerone.

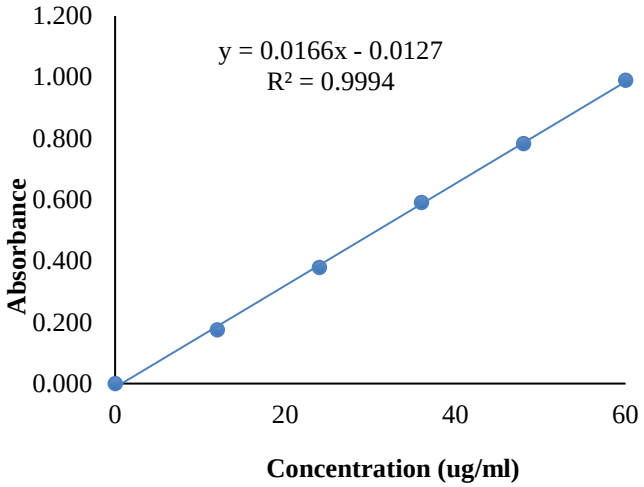

Figure 7: Calibration curve of Zingerone in methanol

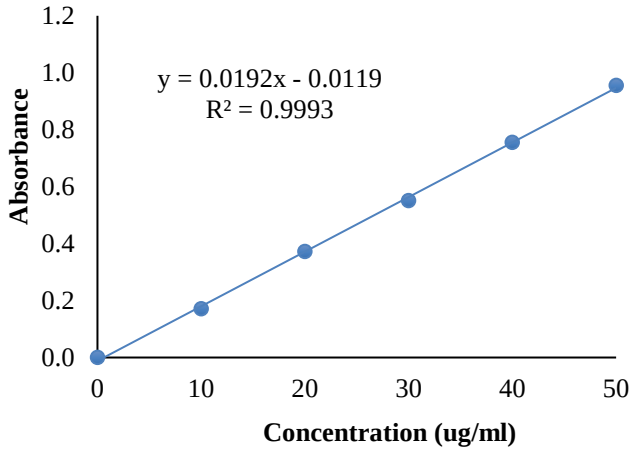

Figure 8: Calibration curve of Zingerone in Phosphate buffer pH 6.4

Table 4: Results of Saturation solubility in different oils

Sr. No.	Sample	Absorbance	Conc (ug/ml)	Dilution	Actual Conc (ug/ml)	Solubility (mg/ml)
1	**Olive Oil**	0.431	26.68	1000	26675.31	26.68
2	**Peanut Oil**	0.891	54.31	1000	54314.27	54.31
3	**Sesame Oil**	0.286	17.96	1000	17963.03	17.96
4	**Isopropyl Myristate**	0.725	44.34	1000	44340.21	44.34
5	**Capryol 90**	0.452	27.94	1000	27937.09	27.94

Formulation and Evaluation of Nanocarriers

Particle Size and Zeta Potential

Formulations F1–F9 displayed particle sizes ranging from 79.7 nm (F4) to 113.9 nm (F2) (Table 5). Statistical evaluation using the Design-Expert software revealed that both oil concentration ($p < 0.0001$) and homogenization speed ($p = 0.0004$) significantly influenced particle size. The predictive regression model demonstrated strong statistical reliability, with $R^2 = 0.9879$, Adjusted $R^2 = 0.9839$, Predicted $R^2 = 0.9744$, and an Adequate Precision value of 39.78. While oil concentration increased particle size, homogenization speed demonstrated an inverse relationship with particle size due to enhanced shear-induced droplet breakup. The final regression equation expressed in terms of actual factors was:

$$\textit{Particle size}\ (nm) = 59.38 + 0.125\ (\textit{Oil concentration}) + 0.0017\ (\textit{Homogenization speed})$$

This equation confirmed the direct proportionality between particle size, oil concentration, and homogenization speed. A close agreement was observed between actual and predicted values, validating the model fit.

The zeta potential values of the nanocarrier formulations ranged from –19.8 mV to –27.3 mV, indicating adequate electrostatic stabilization (Table 8).

Table 5: Particle Size and Zeta Potential of Zingerone-Loaded PLGA Nanocarrier Formulations (Mean ±SD, n = 3)

Sr. No.	Batch	Particle Size(nm)	Z. Potential(mV)
1	F1	90.5 ± 2.1	−23.9 ± 1.2
2	F2	113.9 ± 3.4	−19.8 ± 1.5
3	F3	95.6 ± 2.8	−21.0 ± 1.1
4	F4	79.7 ± 1.9	−27.3 ± 1.3
5	F5	105.2 ± 3.1	−25.2 ± 1.4
6	F6	93.4 ± 2.6	−23.8 ± 1.2
7	F7	99.4 ± 2.9	−21.6 ± 1.3
8	F8	85.2 ± 2.3	−24.8 ± 1.1
9	F9	111.3 ± 3.2	−23.1 ± 1.4

Drug Content and Encapsulation Efficiency

The encapsulation efficiency across different formulations ranged from 95.23% (F2) to 101.99% (F5) (Table 6). This consistently high efficiency indicated minimal drug loss during the fabrication process and successful entrapment of zingerone within the nanocarrier matrix. Values exceeding 100% are attributed to minor analytical and weighing variations and are within acceptable experimental limits.

In Vitro Drug Release

The release profile of zingerone from nanocarriers exhibited an initial burst within the first 0.5–1 h, followed by a sustained

release phase over 4 h. Pure zingerone showed rapid dissolution, reaching approximately 30% release within 4 h. In contrast, nanocarrier formulations demonstrated significantly improved release profiles:

- F1: ~59.6% at 4 h
- F4: ~72.4% at 4 h (highest release)
- F8: ~62.4% at 4 h

(Table 7; Figure 9). Among all tested batches, F4 provided the most favorable sustained-release profile, attributed to its optimized balance of particle size, oil concentration, and polymer distribution.

Table 6: DC of Zingerone-Loaded PLGA Nanocarriers

Sr. No.	Batch	Drug Content (%)(Mean ± SD, n = 3)
1	F1	101.84 ± 0.85
2	F2	95.23 ± 0.72
3	F3	98.83 ± 0.68
4	F4	99.73 ± 0.55
5	F5	101.99 ± 0.91
6	F6	100.64 ± 0.77
7	F7	97.93 ± 0.69
8	F8	98.68 ± 0.63
9	F9	97.78 ± 0.71

Table 7: In vitro drug release profile of zingerone-loaded PLGA nanocarriers (Mean ± SD, n = 3)

Time (hrs)	Pure Drug (%)	F1 (%)	F4 (%)	F8 (%)
0	0.00 ± 0.00	0.00 ± 0.00	0.00 ± 0.00	0.00 ± 0.00
0.5	13.84 ± 0.58	27.39 ± 0.33	32.43 ± 0.30	30.01 ± 0.23
1	18.38 ± 0.37	34.69 ± 0.24	44.48 ± 0.39	41.44 ± 0.11
2	23.50 ± 0.33	46.36 ± 0.33	57.26 ± 0.13	55.35 ± 0.10
3	27.68 ± 0.30	54.56 ± 0.27	66.54 ± 0.25	62.40 ± 0.23
4	30.59 ± 0.33	59.54 ± 0.28	72.43 ± 0.30	68.49 ± 0.19
8	33.44 ± 0.21	65.53 ± 0.38	78.40 ± 0.37	75.52 ± 0.27
12	40.77 ± 0.12	69.63 ± 0.27	82.49 ± 0.11	81.43 ± 0.17
18	48.37 ± 0.24	75.36 ± 0.27	88.56 ± 0.34	86.54 ± 0.18
24	57.69 ± 0.38	84.35 ± 0.28	98.01 ± 0.12	93.15 ± 0.27

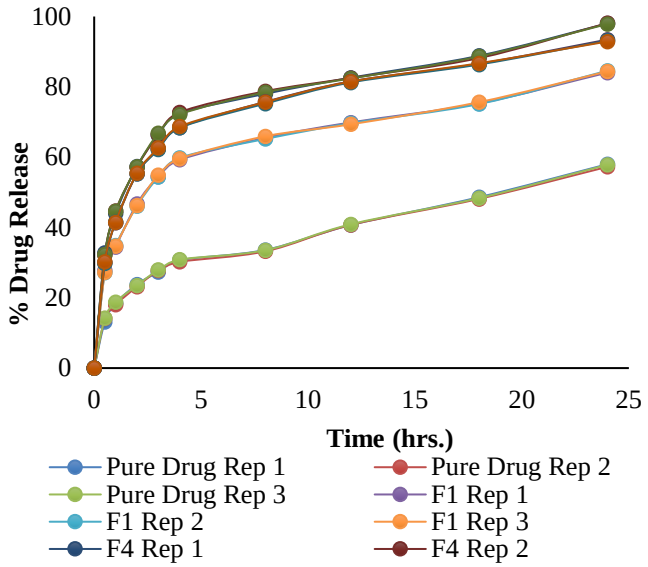

Figure 9: Drug Release studies

Stability Studies

The optimized formulation (F4) was subjected to stability evaluation. No significant variations were noted in terms of particle size, zeta potential, FTIR, DSC thermograms, or drug content after storage. These findings confirmed that the zingerone-loaded PLGA nanocarrier system remained physicochemically stable over the study period.

DISCUSSION

The successful development of zingerone-loaded PLGA nano-carriers was confirmed through comprehensive physicochemical characterization, and the findings are consistent with recent reports on polymeric nanocarriers designed for poorly water-soluble natural compounds [21]. Particle size analysis demonstrated that the prepared nanocarriers were within the nanoscale range of 79.7–113.9 nm, with the optimized batch (F4) exhibiting the smallest mean particle size. Nanoparticles below 200 nm are widely recognized as optimal for enhanced cellular uptake, improved bioavailability, and prolonged systemic circulation due to reduced clearance by the reticuloendothelial system [22]. The negative zeta potential values (–19.8 to –27.3 mV) observed across the formulations indicate sufficient electrostatic repulsion, thereby minimizing particle aggregation and enhancing colloidal stability. Comparable zeta potential values have been reported for PLGA-based nanocarriers encapsulating hydrophobic drugs, confirming that moderately negative surface charges are sufficient to maintain dispersion stability [23].

FTIR analysis confirmed the preservation of zingerone's characteristic functional groups, including O–H, C=O, and aromatic C–H stretching vibrations. The absence of peak

disappearance or significant shifts suggests that the encapsulation process did not chemically modify the drug, indicating physical entrapment within the polymeric matrix. Similar observations have been reported for phenolic phytoconstituents encapsulated in PLGA systems, where drug–polymer compatibility was achieved without chemical interaction. Minor peak shifts suggest weak hydrogen bonding interactions between hydroxyl groups of zingerone and ester groups of PLGA, contributing to sustained drug release behavior [24].

DSC thermograms provided further insight into drug–polymer interactions. The sharp endothermic melting peak of crystalline zingerone was replaced by broadened transitions in the nanocarrier formulations, indicating partial conversion to an amorphous state. Amorphization is known to enhance drug dissolution and molecular dispersion within polymeric carriers, thereby improving the solubility and bioavailability of poorly soluble drugs. Although amorphization enhances solubility, it may compromise long-term stability due to potential recrystallization, necessitating further long-term stability studies [25,26].

SEM analysis revealed that the nanocarriers possessed uniform spherical morphology with smooth surfaces and no visible surface-associated drug crystals. This confirms efficient encapsulation of zingerone within the PLGA matrix & supports the DSC findings indicating reduced crystallinity. Spherical nanocarriers are advantageous for reproducible drug release behavior & predictable biological distribution. The nanocarriers exhibited smooth, non-porous surfaces, which contributed to the initial burst release of surface-associated drug, followed by controlled diffusion through the dense polymer matrix [27].

Preformulation studies established the λmax of zingerone at 282 nm, consistent with reported UV spectral characteristics of phenolic compounds. Calibration curves constructed in methanol and phosphate buffer (pH 6.4) exhibited excellent linearity ($R^2 > 0.99$), confirming the reliability of the spectrophotometric method for quantitative estimation during formulation and release studies [28]. Saturation solubility studies identified peanut oil as the most suitable lipid vehicle for zingerone, with significantly higher solubility than other tested oils. Natural oils have been extensively reported to improve solubilization and serve as efficient carriers for lipophilic bioactives, with their fatty acid composition playing a crucial role in enhancing the molecular dispersion of hydrophobic drugs [29]. Optimization studies using Design-Expert software revealed that both oil concentration and homogenization speed significantly influenced particle size. Increased oil concentration was associated with larger particle size due to the dispersed phase's higher viscosity, which restricts droplet breakup during emulsification. Conversely, higher homogenization speeds promoted efficient shear forces, resulting in smaller particle sizes. These trends are consistent with response surface methodology-based optimization studies reported for polymeric nanocarrier systems. While oil concentration increased particle size, homogenization speed demonstrated an inverse relationship with particle size due to enhanced shear-induced droplet breakup [30-31]. Encapsulation efficiencies exceeding 95% across all formulations indicate minimal drug loss during processing. High encapsulation efficiency is characteristic of PLGA-based systems due to the polymer's hydrophobicity, which provides a favorable microenvironment for lipophilic molecules such as zingerone [32].

In vitro release studies demonstrated biphasic release kinetics characterized by an initial burst followed by sustained release. The initial burst is attributed to the release of surface-associated drug, while sustained release results from diffusion of zingerone through the polymeric matrix. Among all formulations, F4 exhibited the highest release (~72.4% at 4 h), which correlated with its smaller particle size and optimized oil content. Smaller nanoparticles provide increased surface area, facilitating enhanced drug diffusion and release [33]. Additionally, the presence of peanut oil likely enhanced drug partitioning into the aqueous phase, further improving release kinetics [34].

Stability studies confirmed that the optimized formulation (F4) retained particle size, zeta potential, and drug content during storage, indicating satisfactory physicochemical stability. The stability of PLGA nanocarriers has been shown to depend on polymer degradation kinetics and surface charge, with PLGA-based systems demonstrating excellent stability under ambient storage conditions [35]. These findings demonstrate that zingerone-loaded PLGA nanocarriers provide a stable, high-loading, and sustained-release delivery platform. The results align with recent evidence supporting the use of PLGA nanocarriers to enhance the solubility, stability, and bioavailability of poorly water-soluble natural compounds.

CONCLUSION

The present study successfully demonstrated the formulation and characterization of zingerone-loaded PLGA nanocarriers using peanut oil as the preferred lipid phase. The nanocarriers exhibited a nanoscale particle size with adequate zeta potential, confirming colloidal stability. FTIR and DSC analyses verified that no significant chemical interactions occurred between the drug and excipients, while partial amorphization of zingerone enhanced its solubility profile. SEM imaging revealed uniform spherical morphology without surface drug crystals, indicating efficient encapsulation. In vitro release studies showed a biphasic profile, with an initial burst followed by sustained release, highlighting the role of optimized polymer–oil ratios in controlling drug diffusion. Among the tested batches, formulation F4 displayed superior release characteristics and stability during storage. Collectively, these findings confirm that PLGA-based nanocarriers are a promising platform for improving the solubility, stability, and bioavailability of zingerone, and warrant further preclinical evaluation for therapeutic applications. Future work should include in vivo pharmacokinetic evaluation in appropriate rodent models to establish the enhancement of bioavailability and therapeutic relevance.

FINANCIAL ASSISTANCE

NIL

CONFLICT OF INTEREST

The authors declare no conflict of interest.

AUTHOR CONTRIBUTION

Varsha Laxman Jakune and Varsha Sidheshwar Tegeli were responsible for data collection and experimental work. Varsha Laxman Jakune carried out the analytical assessments. Varsha Laxman Jakune prepared the initial draft of the manuscript. All authors reviewed, edited, and approved the final version of the manuscript. All authors contributed to the study conception, design, and interpretation of results.

REFERENCES

[1] Das S, Chaudhury A. Recent advances in lipid nanoparticle formulations with solid matrix for oral drug delivery. *AAPS PharmSciTech*, **12**, 62–76 (2011) https://doi.org/10.1208/s12249-010-9563-0

[2] Nunse D, Shevalkar GB, Borse L. Innovative polymeric micelles with in-situ gelation for enhanced ocular delivery of ketoconazole. *J Pharm Innov*, **20**, 1–12 (2025) https://doi.org/10.1007/s12247-024-09915-w

[3] Danhier F, Ansorena E, Silva JM, et al. PLGA-based nanoparticles: an overview of biomedical applications. *J Control Release*, **161(2)**, 505–522 (2012) https://doi.org/10.1016/j.jconrel.2012.01.043

[4] Meng F, Cheng R, Deng C, Zhong Z. Intracellular drug release nanosystems. *Mater Today*, **15(10)**, 436–442 (2012) https://doi.org/10.1016/S1369-7021(12)70203-9

[5] Sarkar S, Mazumder S, Saha SJ, Bandyopadhyay U. Management of inflammation by natural polyphenols. *Curr Med Chem*, **23(16)**, 1657–1695 (2016) https://doi.org/10.2174/0929867323666160418115540

[6] Patel M, Shah T, Amin A. Lipid-based nanocarriers for bioavailability enhancement of hydrophobic drugs. *AAPS PharmSciTech*, **19(4)**, 1660–1672 (2018) https://doi.org/10.1208/s12249-018-0973-x

[7] Kothawade SN, Pande VV. Formulation and evaluation of amisulpride loaded intranasal microemulsion. *Indian Drugs*, **60(9)**, 1–22 (2023) https://doi.org/10.53879/id.60.09.13783

[8] Pande V, Kothawade S, Kuskar S, et al. Fabrication of mesoporous silica nanoparticles and applications in drug delivery. In: *Nanofabrication Techniques*. IntechOpen (2023) https://doi.org/10.5772/intechopen.112428

[9] Lunkad AS, Agrawal MR, Kothawade SN. Anthelmintic activity of *Bryophyllum pinnatum*. *Res J Pharmacogn Phytochem*, **8(1)**, 21 (2016) https://doi.org/10.5958/0975-4385.2016.00005.4

[10] Kumari A, Yadav SK, Yadav SC. Biodegradable polymeric nanoparticles for drug delivery. *Colloids Surf B Biointerfaces*, **75(1)**, 1–18 (2010) https://doi.org/10.1016/j.colsurfb.2009.09.001

[11] Kothawade SN, Chaudhari PD. Biodegradable porous starch foam for oral delivery of eprosartan mesylate. *J Adv Sci Res*, **12(03)**, 120–126 (2021) https://doi.org/10.55218/JASR.s1202112314

[12] Jain RA. Manufacturing techniques of PLGA drug delivery systems. *Biomaterials*, **21(23)**, 2475–2490 (2000) https://doi.org/10.1016/S0142-9612(00)00115-0

[13] Zhang Y, Chan HF, Leong KW. Advanced nanoparticle delivery systems for natural therapeutics. *Adv Drug Deliv Rev*, **65(4)**, 104–120 (2013) https://doi.org/10.1016/j.addr.2012.07.010

[14] Kothawade SN, Avhad SR, Rngade RB, et al. Aloe vera powder as bioenhancer: a review. *Int J Pharm Phytopharmacol Res*, **13(2)**, 37–44 (2023) https://doi.org/10.51847/ZFFtdBFaPt

[15] Muller RH, Radtke M, Wissing SA. Nanostructured lipid carriers for improved drug solubility. *Adv Drug Deliv Rev*, **54**, 131–155 (2002) https://doi.org/10.1016/S0169-409X(02)00118-7

[16] Hemnani N, Suresh PK. NLC system for ocular drug delivery. *J Appl Pharm Res*, **13**, 141–153 (2025) https://doi.org/10.69857/joapr.v13i3.1162

[17] Yin J, Hou Y, Song X, et al. Polymer-lipid hybrid nanoparticles for oral delivery of quercetin. *Int J Nanomedicine*, **14**, 4045–4057 (2019) https://doi.org/10.2147/IJN.S210057

[18] Pawar MA, Shevalkar GB, Vavia PR. Gastro-retentive delivery system for trazodone. *AAPS PharmSciTech*, **23**, 251 (2022) https://doi.org/10.1208/s12249-022-02404-8

[19] Shevalkar G, Pawar M, Vavia P. NLCs of lumefantrine with enhanced permeation. *J Pharm Innov*, **17**, 1221–1234 (2022) https://doi.org/10.1007/s12247-021-09590-1

[20] Thete R, Shevalkar G, Borse L. NLCs for donepezil nose-to-brain delivery. *Biosci Biotechnol Res Asia*, **21**, 1145–1156 (2024) https://doi.org/10.13005/bbra/3293

[21] Darandale SS, Shevalkar GB, Vavia PR. Lipid composition in propofol formulations. *AAPS PharmSciTech*, **18**, 441–450 (2017) https://doi.org/10.1208/s12249-016-0524-0

[22] Zhao Z, Ukidve A, Kim J, Mitragotri S. Targeting strategies for drug delivery. *Cell*, **181(1)**, 151–167 (2019) https://doi.org/10.1016/j.cell.2019.09.017

[23] Jojo GM, Kuppusamy G, De A, et al. Intranasal nanolipid carriers of pioglitazone. *Drug Dev Ind Pharm*, **45**, 1061–1072 (2019) https://doi.org/10.1080/03639045.2019.1593439

[24] Pawar SK, Vavia PR. Rice germ oil in SMEDDS of tacrolimus. *AAPS PharmSciTech*, **13**, 254–261 (2012) https://doi.org/10.1208/s12249-011-9748-1

[25] Elmowafy M, Al-Sanea MM. NLCs as drug delivery platform. *Saudi Pharm J*, **29**, 999–1012 (2021) https://doi.org/10.1016/j.jsps.2021.07.015

[26] Tamjidi F, Shahedi M, Varshosaz J, et al. NLCs for food bioactives. *Innov Food Sci Emerg Technol*, **19**, 29–43 (2013) https://doi.org/10.1016/j.ifset.2013.03.002

[27] Leng D, Thanki K, Fattal E, et al. Lipid-polymer hybrid nanoparticles engineering. *Int J Pharm*, **548**, 740–746 (2018) https://doi.org/10.1016/j.ijpharm.2017.08.094

[28] Amasya G, Şengel Türk CT, Badilli U, et al. Optimization of SLNs of fluticasone propionate. *Turk J Pharm Sci*, **17**, 359–366 (2020) https://doi.org/10.4274/tjps.galenos.2019.27136

[29] Syed YY. Fluticasone furoate/vilanterol in asthma. *Drugs*, **75**, 407–418 (2015) https://doi.org/10.1007/s40265-015-0354-5

[30] Yadav S, Jain V, Magar H, et al. RP-HPLC method for inhalation formulation. *J Chromatogr Sci*, **62**, 761–766 (2024) https://doi.org/10.1093/chromsci/bmad075

[31] Johnson M. Development of fluticasone propionate. *J Allergy Clin Immunol*, **101**, S434–S439 (1998) https://doi.org/10.1016/S0091-6749(98)70155-1

[32] Giavina-Bianchi P. Fluticasone furoate nasal spray. *Ther Clin Risk Manag*, **4**, 465–472 (2008) https://doi.org/10.2147/TCRM.S1984

[33] Elsisi R, Helal D, Mekhail G, et al. Nanoparticles in skin aging treatment. *Arch Pharm Sci Ain Shams Univ*, **7**, 376–401 (2023) https://doi.org/10.21608/aps.2023.250333.1146

[34] Tavares Luiz M, Santos Rosa Viegas J, Palma Abriata J, et al. DoE in nanoparticle optimization. *Eur J Pharm Biopharm*, **165**, 127–148 (2021) https://doi.org/10.1016/j.ejpb.2021.05.011

[35] Tang C, Niu X, Shi L, et al. Pharmacokinetic drug-drug interaction study. *Front Pharmacol*, **11** (2021) https://doi.org/10.3389/fphar.2020.626897